Systematic Investigation of Alkali Metal Ion Transfer Across the Micro- and Nano-Water/1,2-Dichloroethane Interfaces Facilitated by Dibenzo-18-crown-6

Yi Yuan and Yuanhua Shao*

State Key Laboratory of Electroanalytical Chemistry, Changchun Institute of Applied Chemistry, Chinese Academy of Sciences, Changchun 130022, China

Received: September 25, 2001; In Final Form: January 3, 2002

Facilitated alkali metal ion (M^+= Li^+, Na^+, K^+, Rb^+, and Cs^+) transfers across the micro- and nano-water/1,2-dichloroethane (W/DCE) interfaces supported at the tips of micro- and nanopipets by dibenzo-18-crown-6 (DB18C6) have been investigated systematically using cyclic voltammetry. The theory developed by Matsuda et al. was applied to estimate the association constants of DB18C6 and M^+ in the DCE phase based on the experimental voltammetric results. The kinetic measurements for alkali metal ion transfer across the W/DCE interface facilitated by DB18C6 were conducted using nanopipets or submicropipets, and the standard rate constants (k^0) were evaluated by analysis of the experimental voltammetric data. They increase in the following order: $k^0_{Cs^+} < k^0_{Li^+} < k^0_{Rb^+} < k^0_{Na^+} < k^0_{K^+}$, which is in accordance with their association constants except Cs^+ and Li^+.

Introduction

Complexation reactions between metal ions and ionophores at a liquid/liquid (L/L) interface or an interface between two immiscible electrolyte solutions (ITIES) have attracted much attention due to the wide range of applicability of these systems in chemistry and biology.[1] Since the pioneering work of Koryta et al. on the facilitated potassium ion transfer across the water/nitrobenzene (W/NB) interface by valinomycin and dibenzo-18-crown-6 (DB18C6),[2] extensive studies on thermodynamics have been carried out on a larger number of neutral or synthetic macromolecules, which are able to form a complex with alkali metal ions at a L/L interface.[3−10] The problems arising from charge current and resistive effect can be effectively overcome by placing one of two liquid phases in a microsized pipet[11] or supporting an interface on the microhole of a thin polymer film[12−14] to construct a micro-L/L interface. Micropipet voltammetry, first introduced by Taylor and Girault,[11a] has been successfully employed to study thermodynamics and kinetics of various electron transfer (ET) and ion transfer (IT) processes.[11] Recently, a nano-L/L interface supported at a nanopipet was used to measure the kinetic parameter for facilitated potassium ion transfer by DB18C6 across the W/DCE interface.[15a]

Although there have been many reports on the facilitated ion transfer by DB18C6, few systematic studies of alkali metal ion transfer across a L/L interface facilitated by this crown ether have been reported,[7,9] especially the kinetics of the facilitated ion transfer (FIT) process. In the present work, our primary goal is to study the thermodynamics and kinetics of facilitated alkali metal ion transfer across the W/DCE interface using micro- and nanopipets. In addition, we also try to explore the relationship between the association constants and transfer kinetics.

Experimental Section

Chemicals. Lithium chloride (LiCl), potassium chloride (KCl), sodium chloride (NaCl), rubidium chloride (RbCl), cesium chloride (CsCl), dibenzo-18-crown-6 (DB18C6), tetramethylammonium chloride (TMACl), and 1,2-dichloroethane (DCE) were obtained from Beijing Chemical Co.. Tetrabutylammonium chloride (TBACl) and potassium tetrakis(4-chlorophenyl)borate (KTPBCl) were purchased from Aldrich. The organic phase supporting electrolyte, tetrabutylammonium tetrakis(4-chlorophenyl)borate (TBATPBCl), was prepared and purified using the procedures described previously.[16] All reagents were of analytical grade and used without further purification. Ultrapure water obtained from a Millipore Milli-Q water purification system was used throughout the experiments. Special cautions were taken for dealing with DCE and other hazardous chemicals.

Fabrication of Micro- and Nanopipets. Micropipets were made from borosilicate glass capillaries (o.d./i.d. = 1.0 mm/0.58 mm, L = 10 cm) and nanopipets were from quartz glass capillaries with filament (o.d./i.d. = 1.0 mm/0.70 mm, L = 10 cm) using a Model P-2000 laser-based puller (Sutter Instrument Co.). The appropriate pulling programs were selected to fabricate patch-type micropipets in order to minimize the *iR* drop inside the narrow shaft. All prepared micropipets were inspected using an Olympus BX-60 optical microscope (×100 to ×500, Japan) before experiments. Aqueous solutions were infused into the pipets from the back with a small syringe (10 μL).

Electrochemical Measurements. A computer-controlled BAS 100 B/W Electrochemical Workstation (Bioanalytical Systems) was used for voltammetric studies. A two-electrode setup previously described by Beattie et al. was employed in the experiments.[11b] Two Ag/AgCl electrodes were separately inserted into the aqueous phase inside a micropipet or nanopipet and the organic phase reference solution. All electrochemical experiments were performed at 22 ± 1 °C. The Galvani potential difference ($\Delta^w_o\phi = \phi^w - \phi^o$, ϕ^w and ϕ^o are the inner Galvani potentials of the aqueous phase and the organic phase, respectively) is related to E by

$$E = \Delta^w_o\phi - \Delta^w_o\phi^{0'}_{TBA^+} \quad (1)$$

* To whom the correspondence should be addressed. E-mail: yhshao@ns.ciac.jl.cn.

10.1021/jp015548m CCC: $22.00
Published on Web 07/18/2002

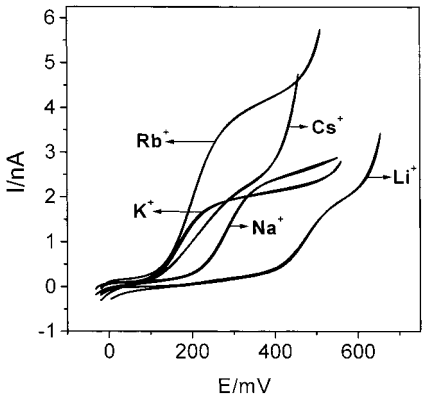

Figure 1. Steady-state voltammograms for alkali metal ion transfer across the W/DCE interface facilitated by DB18C6. Experimental conditions see cell 1. $x = 0.1$ M. The radii of the micropipets for Li^+, Na^+, K^+, Rb^+, and Cs^+ are 12, 9, 8, 16, and 8 μm, respectively; scan rate 100 mV s^{-1}.

where the formal potential for TBA^+ ($\Delta_o^w\phi^{0'}_{TBA^+}$) can be expressed as

$$\Delta_o^w\phi^{0'}_{TBA^+} = \Delta_o^w\phi^{0}_{TBA^+} + \frac{RT}{zF}\ln\left(\frac{\gamma^\circ_{TBA^+}}{\gamma^w_{TBA^+}}\right) \qquad (2)$$

where the standard potential for TBA^+, $\Delta_o^w\phi^{0}_{TBA^+} = -230$ mV across the W/DCE interface on the TATB (tetraphenylarsonium tetraphenylborate) scale.[17] A positive current refers to the transfer of cation from the aqueous to the organic phase or anion from the organic to the aqueous phase, whereas a negative current refers to the transfer of cation from the organic to the aqueous phase or anion from the aqueous to the organic phase.

Results and Discussion

Estimation of Diffusion Coefficient and Mechanism of Facilitated Alkali Metal Ion Transfer by DB18C6. The following electrochemical cell 1 was employed for investigation of alkali metal ion transfer across the micro-W/DCE interface facilitated by DB18C6,

where M is Li, Na, K, Rb, or Cs, respectively.

Figure 1 presents steady-state voltammograms for the transfer of Li^+, Na^+, K^+, Rb^+, and Cs^+ ions across the W/DCE interface facilitated by DB18C6 using micropipets with different radii. As described by Stewart et al., simple IT reactions at a micropipet are characterized by an asymmetric diffusion regime.[11c] The transfer of ions out of the pipet (egress transfer) controlled by linear diffusion leads to a peak-shaped current response, whereas transfer into the pipet (ingress transfer) controlled by diffusion of a spherical (or hemispherical) type produces a steady-state wave. The obtained steady-state currents are consistent with the asymmetric diffusion regime formed at the interface due to the specific shape of the micropipet. During the forward scan, alkali metal ion transfer from the aqueous phase inside a micropipet to the outer DCE phase is facilitated by DB18C6, which is controlled by spherical diffusion of DB18C6 to the interface, and the reverse process is dominated by the same diffusion manner of the complexed ion $(M-DB18C6)^+$. On the condition that the concentrations of alkali metal ions are much higher than that of DB18C6, the steady-state cyclic voltammograms for forward and backward scans demonstrate that the transfer mechanism for facilitated alkali metal ions across the W/DCE interface by DB18C6 is shown to be a transfer by interfacial complexation (TIC) and interfacial dissociation (TID).[11d]

According to Beattie et al., the behavior of a micro-W/DCE interface supported at the tip of a micropipet exhibits behavior between that of a microhemisphere and that of a microsphere.[11b] The steady-state current obeys the following equation

$$I_{ss} = 3.35\pi nFD^\circ ca \qquad (3)$$

where I_{ss} is the steady-state current, D° is the diffusion coefficient of ionophore in the DCE phase, n is the charge number, F is the Faraday constant, c is the bulk concentration of the ionophore, and a is the internal radius of pipet. The diffusion coefficients of DB18C6 in the DCE phase are obtained from eq 3 and are approximately equal to 5.25×10^{-6}, 5.19×10^{-6}, 4.88×10^{-6}, 5.01×10^{-6}, and 5.60×10^{-6} cm^2 s^{-1} with the supporting electrolytes LiCl, NaCl, KCl, RbCl, and CsCl, respectively. The mean value of the diffusion coefficient of DB18C6 in DCE phase is $(5.19 \pm 0.34) \times 10^{-6}$ cm^2 s^{-1}, which is close to the literature result.[18]

Evaluation of the Association Constants in the DCE Phase under DB18C6 Diffusion-Controlled Process. Ion transfer voltammetry is also a very effective method to obtain thermodynamic data (association constant, stoichiometric parameter, etc.) from the study of concentration dependence on the half-wave potential. According to Matsuda et al., if the concentration of the metal ion in the aqueous phase ($c^w_{M^+}$) is in excess compared with the concentration of the ionophore in the organic phase (c^o_L), which can be distributed between the two phases, the following condition is fulfilled:[19]

$$1 + \xi K_{DL} \geq 20\beta^w c_{M^+} \qquad (4)$$

where $K_{DL}(c^o_L/c^w_L)$ is the partition coefficient of the ionophore and ξ is the square root of the diffusion coefficients in the organic and the aqueous phases, respectively. β^w is the association constant in the aqueous phase. Then the half-wave potential of the complex $(M-L)^+$ is given by

$$\Delta_o^w\phi_{1/2} = \Delta_o^w\phi^{0'}_{M^+} + \frac{RT}{2zF}\ln\left(\frac{D_L}{D_{ML^+}}\right)^{1/2} - \frac{RT}{zF}\ln(\beta_1^\circ c^w_{M^+}) \qquad (5)$$

where $\Delta_o^w\phi^{0'}_{M^+}$ is the formal potential of metal ion transfer. D_L and D_{ML^+} are the diffusion coefficients of ionophore and ion−ionophore complex, respectively. β_1° is defined as the association constant in the organic phase. D_L and D_{ML^+} are approximately equal due to the large size of the ionophore DB18C6 with respect to alkali metal ions; thus eq 5 can be reduced to

$$\Delta_o^w\phi_{1/2} = \Delta_o^w\phi^{0'}_{M^+} - \frac{RT}{zF}\ln(\beta_1^\circ c^w_{M^+}) \qquad (6)$$

A study of concentration dependence on the half-wave potential is carried out to evaluate the association constants of the $(M-DB18C6)^+$ complexes in the DCE phase. Figure 2 shows steady-state voltammograms of the facilitated lithium ion transfer across the micro-W/DCE interface by DB18C6 under various concentrations of LiCl. It is obvious that the half-wave potential shifts negatively with the increasing concentration of LiCl. The plots of the half-wave potentials versus the logarithm of all alkali metal ion concentrations in the aqueous phase are shown in

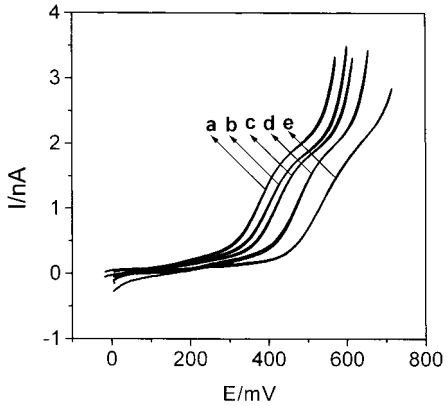

Figure 2. Steady-state voltammograms for Li^+ transfer across the W/DCE interface facilitated by DB18C6 at various LiCl concentrations. *x* is (a) 0.7 M, (b) 0.5 M, (c) 0.3 M, (d) 0.1 M, and (e) 0.05 M in cell 1. Scan rate: 100 mV s^{-1}. Radius of the micropipet: 12 μm.

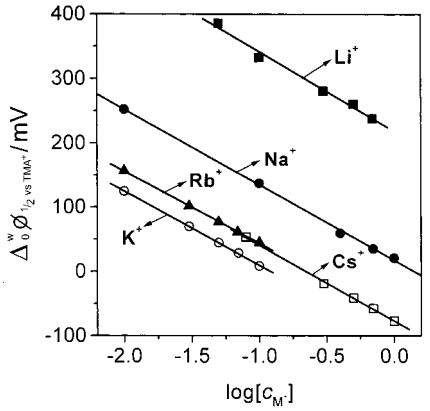

Figure 3. Dependence of $\Delta_o^w\phi_{1/2vsTMA^+}$ on the logarithm of the concentration of M^+ ion using cell 1. M is Li, Na, K, Rb, and Cs, respectively.

Figure 3. The half-wave potential of each alkali metal ion is evaluated in accordance with the TATB assumption in the form

$$\Delta_o^w\phi_{M^+}^{0'} = \Delta_o^w\phi_{1/2,M^+(exp)} - [\Delta_o^w\phi_{1/2,TMA^+(exp)} - \Delta_o^w\phi_{TMA^+}^{0'}] \quad (7)$$

where the formal transfer potential of TMA^+, $\Delta_o^w\phi_{TMA^+}^{0'}$ is 160 mV.[20] Clearly, the plot for Li^+ gives a straight line with a reciprocal slope of -123 ± 2 mV $decade^{-1}$ and an intercept of 0.219 V. Given that the potential of silver/silver chloride electrode inside the micropipet varies with the concentration of chloride ion in the aqueous phase, a 1:1 complex, $(Li-DB18C6)^+$, is formed at the interface. According to eq 6, the logarithm of the association constant of the $(Li-DB18C6)^+$ complex in the DCE phase ($\log \beta_1^o$) is determined to be 6.13 on the basis of $\Delta_o^w\phi_{Li^+}^{0'} = 576$ mV.[17] Similarly, the logarithm of the association constant ($\log \beta_1^o$) for other alkali metal ions, such as Na^+, K^+, Rb^+, and Cs^+, are determined to be 9.66, 11.07, 9.36, and 7.96, respectively, on the basis of the formal transfer potential $\Delta_o^w\phi_{M^+}^{0'}$ of corresponding alkali metal ions.[17] From the experimental results, the selectivity of DB18C6 toward the alkali metal ions follows the sequence of $Li^+ < Cs^+ < Rb^+ < Na^+ < K^+$. Table 1 lists the relevant data and experimental results about the complexation reactions between DB18C6 and alkali metal ions in the DCE solution. Previous thermodynamic data suggest that the stability of macrocyclic complexes depend on the relative cation and ligand binding sites, the number and spatial arrangements of the ligand binding sites,

TABLE 1: Ion Radius (*r*), Formal Transfer Potential ($\Delta_o^w\phi^{0'}$) of Relevant Alkali Metal Ions and the Association Constants of Complex $(M\text{-}DB18C6)^+$ in the DCE Phase

ion	*r* (Å)	$\Delta_o^w\phi_{M^+}^{0'}$[a]/mV	$\Delta_o^w\phi_{ML^+}^{0'}$/mV	$\Delta\Delta_o^w\phi^{0'}$/mV	$\log \beta_{ML^+}^o$
Li^+	0.76	576	332.9	243.1	6.13
Na^+	1.02	579	137.1	441.9	9.66
K^+	1.38	538	8.6	529.4	11.07
Rb^+	1.52	475	44.8	430.2	9.36
Cs^+	1.67	386	42.2	343.8	7.96

[a] from the literature.[17]

the substitution on the macrocyclic ring, and the solvent effects.[21] The size-fit theory is more suitable for the case of the complexation between ionophore and metal ion. According to the theory, the metal ion can be positioned in the center of the ligand cavity or in the ligand plane with optimal metal ion−donor atom distances when the size of the ionophore cavity matches that of metal ion, which results in maximal complex stability.[22] With regard to cavity size considerations, DB18C6 possesses a cavity of 2.9 ± 0.3 Å in diameter. The potassium ion having an ionic diameter of 2.76 Å would therefore be the highest selectivity toward this crown ether. DB18C6 can complex with Na^+ and Rb^+ ion with high selectivity because their radii are close to the cavity size of DB18C6. However, the radii of Li^+ and Cs^+ are too small or large compared with the cavity size of DB18C6. Hence, it is reasonable that DB18C6 exhibits high selectivity for K^+, Rb^+, and Na^+ but not for Li^+ and Cs^+. Certainly, the selectivity toward metal ion is also affected by other factors including the solvation patterns of the species involved, ligand conformation before and after complexation, and the number and nature of the chelate rings formed upon complexation. Samec et al.[7] reported previously the systematic studies of the thermodynamics of alkali metal ion transfer facilitated by DB18C6, DB24C8, and DB30C10; the selectivity sequence for DB18C6 in DCE is $Cs^+ < Rb^+ < Na^+ < K^+ < Li^+$, which is different from our results. They thought that the dominating factor was the change of cation solvation but not cavity size effect. The problem in their work was that the values of the estimated formal potential of metal ions were wrong and this was corrected in their following work.[9]

Kinetic Measurements for Alkali Metal Ions Transfer Across the Micro-W/DCE Interface Facilitated by DB18C6. During the last two decades, several groups have tried to measure the rate constant for facilitated K^+ ion transfer from water to DCE by DB18C6. Previous measurements at large L/L interfaces (mm in size) were influenced by resistive and capacitive effects.[23,24] The studies reported by Girault et al. indicated that k^0 is inaccessible when impedance spectroscopy and steady-state voltammetry are employed at a micro-L/L interface.[11b,g] Later, the lower limit for $k^0 > 0.5$ cm s^{-1} was obtained from pulse voltammetry at a micro-L/L interface.[24] The application of steady-state voltammetry at ultramicroelectrodes to the measurement of rapid heterogeneous ET kinetics has been discussed previously,[25,26] and the developed methodologies are applicable to IT assuming that the potential dependence of the rate constant follows the Bulter−Volmer equation.[1a,11b] The kinetic parameters of the electrode reaction can be evaluated from steady-state voltammogram by the three-point method, i.e., the half-wave potential, $E_{1/2}$, and two quartile potentials, $E_{1/4}$ and $E_{3/4}$. A single table containing the above parameters for all possible pairs of $\Delta E_{1/4} = E_{1/2} - E_{1/4}$ and $\Delta E_{3/4} = E_{3/4} - E_{1/2}$ is suitable for any kind of uniformly accessible electrode.[15a] This method also provides two useful diagnostic criteria: (i) reliable kinetic parameters can only be obtained if $\Delta E_{1/4} \geq 30.5$ mV and $\Delta E_{3/4} \geq 31$ mV (otherwise,

TABLE 2: Kinetic Parameters for Alkali Metal Ion Transfer Facilitated by DB18C6

Li^+	a/nm	75	154	606	796	898
	α	0.69	0.77	0.66	0.38	0.44
	k^0/cm s^{-1}	0.59	0.66	0.11	0.23	0.22
Na^+	a/nm	20	31	222	253	320
	α	0.79	0.79	0.46	0.17	0.46
	k^0/cm s^{-1}	1.72	1.11	1.46	0.91	1.01
K^+	a/nm	31	63	118	159	173
	α	0.79	0.77	0.59	0.59	0.59
	k^0/cm s^{-1}	1.72	1.62	2.15	1.62	1.47
Rb^+	a/nm	37	53	455	466	595
	α	0.79	0.75	0.46	0.53	0.53
	k^0/cm s^{-1}	1.14	0.94	0.71	0.44	0.34
Cs^+	a/nm	132	145	155	355	383
	α	0.70	0.66	0.67	0.60	0.66
	k^0/cm s^{-1}	0.37	0.24	0.20	0.16	0.12

the cyclic voltammogram is essentially Nernstian, that is, a diffusion controlled process); (ii) the inequality $|\Delta E_{3/4}| \geq |\Delta E_{1/4}|$ holds true for any undistorted quasi-reversible voltammogram. The kinetic parameters can be found from the literature[26] for given values of $\Delta E_{1/4}$ and $\Delta E_{3/4}$, the standard rate constant (k^0) is given by

$$k^0 = \frac{\lambda D^\circ}{a} \tag{8}$$

where k^0, D°, and a have been defined in the context and parameter λ can be obtained from the literature.[26] This method has been successfully employed for evaluating the standard rate constant of facilitated potassium ion transfer across the W/DCE interface by DB18C6.[15a] In this paper, we employ a similar way to systematically study the kinetics for alkali metal ions facilitated by DB18C6 across the W/DCE interface. Both nonsilanized and silanized nanopipets were employed to do the kinetic measurements. The silanization method is the same as shown in our previous work,[15b] and it is extremely difficult to silanize only the outer walls of the nanopipets when their radii are smaller than 100 nm because the capillary action is bigger than the force caused by gas passing through it. Nevertheless, the standard rate constants measured by silanized nanopipets are essentially similar to the data by nonsilanized pipets (see Table 3). Under these conditions, the nano-L/L interfaces can be assumed to be a flat interface. The equation to obtain the effective radius is the same as the eq 7 in the ref 15c for the case of RG = 1.1, which is different from nonsilanized cases.

Figures 4−7 are background-subtracted steady-state voltammograms for facilitated Li^+, Na^+, Rb^+, and Cs^+ ion transfer across the W/DCE interface by DB18C6, respectively. The background-subtracted steady-state voltammograms are obtained as described previously. It is obvious that these curves are almost completely retraceable and all possess well-defined, flat plateaus and baselines. The values of $\Delta E_{1/4}$ and $\Delta E_{3/4}$ can be easily obtained from steady-state voltammograms. The radii of nanopipets are obtained according to eq 3. As discussed above, k^0 can be calculated from eq 8. A number of voltammograms at different sized nanopipets yield similar values of the standard rate constant, and the experimental results are listed in Table 2. The mean value of k^0 for facilitated Li^+, Na^+, K^+, Rb^+, and Cs^+ ion transfer across the W/DCE interface are determined to be 0.38 ± 0.24, 1.24 ± 0.34, 1.71 ± 0.26, 0.71 ± 0.33, and 0.22 ± 0.10 cm s^{-1}, respectively. The transfer coefficients (α)

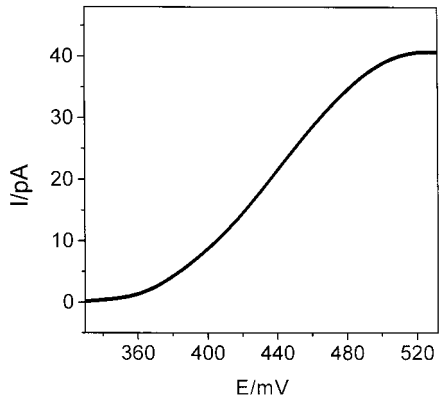

Figure 4. Background-subtracted steady-state voltammogram for Li^+ using cell 1. c_{LiCl} = 0.3 M; scan rate 100 mV s^{-1}; radius of nanopipet 158 nm.

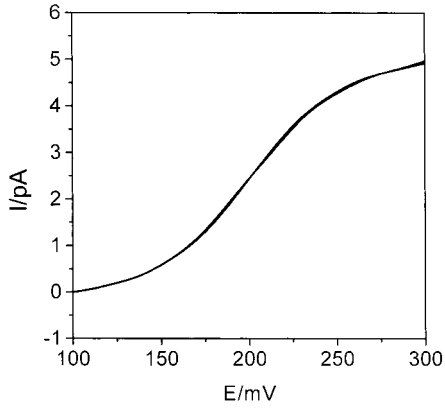

Figure 5. Background-subtracted steady-state voltammogram for Na^+ using cell 1. c_{NaCl} = 1.0 M; scan rate 100 mV s^{-1}; radius of nanopipet 20 nm.

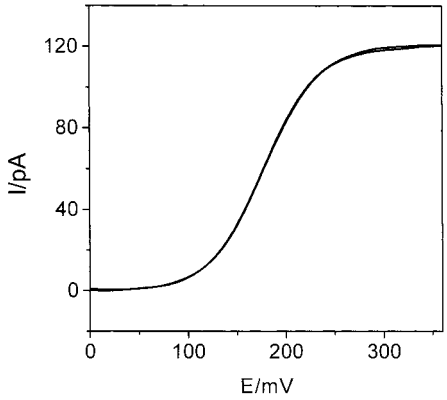

Figure 6. Background-subtracted steady-state voltammogram for rubidium ion using cell 1. c_{RbCl} = 0.1 M; scan rate 100 mV s^{-1}; radius of nanopipet 455 nm.

TABLE 3: Mean Kinetic Parameters for Alkali Metal Ion Transfer Facilitated by DB18C6

	Li^+	Na^+	K^+	Rb^+	Cs^+
k^0/cm s^{-1} [a]	0.38 ± 0.24	1.24 ± 0.34	1.71 ± 0.26	0.71 ± 0.33	0.22 ± 0.10
α[a]	0.59 ± 0.17	0.53 ± 0.26	0.67 ± 0.10	0.61 ± 0.15	0.66 ± 0.04
k^0/cm s^{-1} [b]	0.34 ± 0.20	0.94 ± 0.37	1.73 ± 0.49	0.68 ± 0.20	0.29 ± 0.05
α[b]	0.83 ± 0.17	0.36 ± 0.08	0.54 ± 0.24	0.55 ± 0.24	0.45 ± 0.08

[a] By nonsilanized pipets. [b] By silanized pipets (obtained from Table 2 in ref 26).

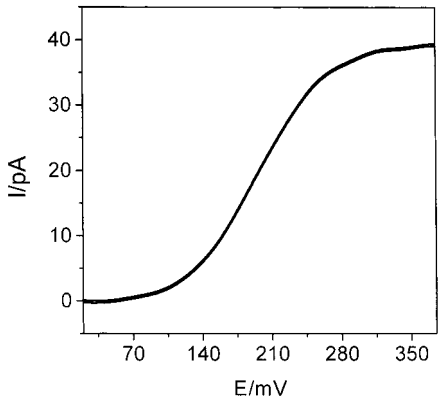

Figure 7. Background-subtracted steady-state voltammogram for cerium ion using cell 1. $c_{CsCl} = 0.08$ M; scan rate 100 mV s^{-1}; radius of nanopipet 155 nm.

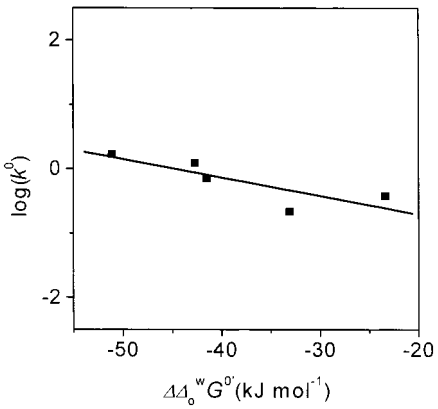

Figure 8. Plot of log(k^0) versus $\Delta\Delta_o^w G^{0'}$.

are determined to be 0.59 ± 0.17, 0.53 ± 0.26, 0.67 ± 0.10, 0.61 ± 0.15, and 0.66 ± 0.04, respectively.

The driving force for alkali metal ion transfer across the W/DCE interface facilitated by DB18C6 should depend on the difference of the Gibbs energy of transfer between the simple ion and complexed ion, that is

$$\Delta\Delta_o^w G^{0'} = -nF(\Delta_o^w \phi_{M^+}^{0'} - \Delta_o^w \phi_{ML^+}^{0'}) \quad (9)$$

Although Marcus recently formulated the theory for an ion transfer reaction at a L/L interface and proposed a mechanism involving initial desolvation of an ion from the first phase, A, and concerted solvation by the second phase, B, we do believe that a simple IT process is different from a FIT process.[27] Consider the cases of an ET process and a FIT reaction at a L/L interface; it is not difficult to find out that there are some similarities between them.[28] For instance, the two species on either side of a L/L interface (one species of the redox couple from both phases in an ET case or an ionophore and an ion in a FIT case) have to diffuse to the interface to have an ET (or complexation) process. In this regard, we think that a FIT is more like an ET process. In our cases, the concentrations of the alkali metal ions are much higher than that of the ionophore; the diffusion of the ionophore to the interface is similar to that of the usual ET process where the concentration of a redox couple in one phase (usually in the aqueous phase) is much higher than that in another phase. This can simplify the data analysis because for the ET reaction one of the phases with higher concentration can be treated as a metal phase.[29] There has been no report so far to treat a FIT process by the Marcus formulation;[30] therefore, it is not clear whether this kind of FIT can be analyzed by means of this theory. Nevertheless, it is true the experimental kinetic data can be analyzed by either Butler−Volmer (B−V) theory or by Marcus formulization depending upon the magnitude of the driving force. Schmicker recently treated a FIT process using a simple lattice-gas model and emphasized the potential drop affecting the concentration of the reactants at the phase boundary.[28]

Figure 8 is the plot of the logarithm of the experimental standard rate constants versus $\Delta\Delta_o^w G^{0'}$. It is roughly a straight line, which may follow the B−V theory since the driving force is not very high. Indeed, these data and analysis are rather preliminary and further understanding of this matter is in progress in our lab.

Conclusions

We have applied micro- and nanopipets and steady-state cyclic voltammetry to investigate systematically the thermodynamics and kinetics of alkali metal ion transfer across the W/DCE interface facilitated by DB18C6. The association constants for alkali metal ions with this ionophore were evaluated according to the theory presented by Matsuda et al. and obey the following order: $Li^+ < Cs^+ < Rb^+ < Na^+ < K^+$. The standard rate constants (k^0) were measured by use of submicropipets and nanopipets voltammetry based on the method developed by Mirkin and Bard. They increase in the following order: $k^0_{Cs^+} < k^0_{Li^+} < k^0_{Rb^+} < k^0_{Na^+} < k^0_{K^+}$. It is obvious that the transfer rate and the association constant are both consistent with the size-fit theory to some extent. The standard rate constants for facilitated alkali metal ion transfer are fast (0.1−2 cm s^{-1}) and measurable.

Acknowledgment. We acknowledge the Chinese Academy of Sciences, the National Natural Science Foundation of China (NSFC, No. 29825111), the Third World Academy of Sciences, and the State Key Laboratory of Electroanalytical Chemistry for the financial supports.

References and Notes

(1) (a) Girault, H. H. In *Modern Aspect of Electrochemistry*; Bockris, J. O., Conway, B. E., White, R. E., Eds.; Plenum Press: New York, 1993; Vol. 15, p 31. (b) Koryta, J. *Electrochim. Acta* **1987**, *32*, 419. (c) Freiser, H. *Chem. Rev.* **1988**, *88*, 611. (d) Dietz, M. L.; Freiser, H. *Langmuir* **1991**, *7*, 284. (e) Buhlmann, P.; Pretsch, E.; Bakker, E. *Chem. Rev.* **1998**, *98*, 1593.

(2) Koryta, J. *Electrochim. Acta* **1979**, *24*, 293.

(3) Sabela, A.; Koryta, J.; Valent, O. *J. Electroanal. Chem.* **1986**, *204*, 267.

(4) Yoshida, Z.; Kihara, S. *J. Electroanal. Chem.* **1987**, *227*, 171.

(5) Dassie, S. A.; Yudi, L. T.; Baruzzi, A. M. *J. Electroanal. Chem.* **1999**, *464*, 54.

(6) Wickens, J.; Dryfe, R. A. W.; Mair, F. S.; Pritchard, R. G.; Hayes, R.; Arrigan, D. W. M. *New J. Chem.* **2000**, *24*, 149.

(7) Samec, Z.; Papoff, P. *Anal. Chem.* **1990**, *62*, 1010.

(8) Campbell, J. A. Ph.D. Thesis, Edinburgh University, Edinburgh, 1991.

(9) Sabela, A.; Marecek, Z.; Samec, Z, Fuoco, R. *Electrochim. Acta* **1992**, *137*, 231.

(10) Hundhammer, R.; Solomon, T.; Zerihun, T.; Abegaz, M.; Bekele, A.; Graichen, K. *J. Electroanal. Chem.* **1994**, *371*, 1.

(11) (a) Taylor, G.; Girault, H. H. *J. Electroanal. Chem.* **1986**, *208*, 179. (b) Beattie, P. D.; Delay, A.; Girault, H. H. *J. Electroanal. Chem.* **1995**, *380*, 167. (c) Stewart, A. A.; Shao, Y.; Pereira, C. M.; Girault, H. H. *J. Electroanal. Chem.* **1994**, *305*, 135. (d) Shao, Y.; Osborne, M. D.; Girault, H. H. *J. Electroanal. Chem.* **1991**, *318*, 101. (e) Shao, Y.; Girault, H. H. *J. Electroanal. Chem.* **1992**, *334*, 203. (f) Campbell, J. A.; Stewart, A. A.; Girault, H. H. *J. Chem. Soc., Faraday Trans.* **1989**, *85*, 843. (g) Battie, P. D.; Delay, A.; Girault, H. H. *Electrochim. Acta* **1995**, *40*, 2961.

(12) (a) Campbell, J. A.; Girault, H..H. *J. Electroanal. Chem.* **1989**, *266*, 465. (b) Osborne, M. D.; Shao, Y.; Pereira C. M.; Girault, H. H. *J. Electroanal. Chem.* **1994,** *364*, 155. (c) Wilke, S.; Osborne, M. D.; Girault, H. H. *J. Electroanal. Chem.* **1997**, *436*, 53.

(13) Pereira, C. M.; Silva, F. *Electroanalysis* **1994**, *6*, 1034.

(14) Wilke, S.; Zerihun, T. *Electrochim. Acta* **1998**, *44*, 15.
(15) (a) Shao, Y.; Mirkin, M. V. *J. Am. Chem. Soc.* **1997**, *119*, 8103. (b) Shao, Y.; Mirkin, M. V. *Anal. Chem.* **1998**, *70*, 3155. (c) Shao, Y.; Mirkin, M. V. *J. Phys. Chem. B* **1998**, *102*, 9915.
(16) Shao, Y.; Girault, H. H. *J. Electroanal. Chem.* **1990**, *282*, 59.
(17) Shao, Y.; Steawart, A. A.; Girault, H. H. *J. Chem. Soc., Faraday Trans.* **1991**, *87*, 2593.
(18) Lin, S.; Zhao, Z.; Freiser, H. *J. Electroanal. Chem.* **1986**, *210*, 137.
(19) Matsuda, H.; Yamada, Y.; Kanamori, K.; Kudo, Y.; Takeda, Y. *Bull. Chem. Soc. Jpn.* **1991**, *64*, 1497.
(20) Wandlowski, T.; Marecek, V.; Samec, Z. *Electrochim. Acta* **1990**, *35*, 1173.
(21) Izatt, R. M.; Bradshaw, J. S.; Nieisen, S. A.; Lamb, J. D.; Sen, D.; Christensen, J. J. *Chem. Rev.* **1985**, *85*, 271.
(22) Brandshaw, J. S.; Izatt, R. M.; Bordunov, A. V.; Zhu, C. Y.; Hathaway, J. K. In *Comprehensive Supramolecular Chemistry*; Lehn. J. M., Ed.; Pergamon: Oxford, U.K., 1996; Vol. 1, p 65.
(23) Kakiuchi, T.; Nishiwakim, Y.; Osakai, T.; Senda, M. *Bull. Chem. Soc. Jpn.* **1986**, *56*, 781.
(24) Tokuda, K.; Kitamura, F.; Liao, Y.; Okuwaki, M.; Ohsaka, T. *In Charge Transfer at Liquid/Liquid and Liquid/Membrane Interface*, Koyto, 1996, p 7.
(25) Oldham, K. B.; Myland, J. C.; Zoski, C. G.; Bond, A. M. *J. Electroanal. Chem.* **1989**, *270*, 79.
(26) Mirkin, M. V.; Bard, A. J. *Anal. Chem.* **1992**, *64*, 2293.
(27) Marcus, R. A. *J. Chem. Phys.* **2000**, *113*, 1618.
(28) Schmickler, W. *J. Electroanal. Chem.* **1999**, *460*, 144.
(29) (a) Samec, Z. *J. Electroanal. Chem.* **1979**, *103*, 1. (b) Geblewicz, G.; Schiffrin, D. J. *J. Electroanal. Chem.* **1988**, *244*, 27. (c) Stewart, A. A.; Campbell, J. A.; Girault, H. H.; Eddowes, M. *Ber. Bunsen-Ges. Phys. Chem.* **1990**, *94*, 83.
(30) (a) Marcus, R. A. *J. Chem. Phys.* **1965**, *43*, 679. (b) Marcus, R. A. *J. Phys. Chem.* **1990**, *94*, 1050. (c) Marcus, R. A. *J. Phys. Chem.* **1991**, *95*, 2010.